J|A|C|S COMMUNICATIONS

Published on Web 03/15/2010

Surface Junction Effects on the Electron Conduction of Molecular Wires

Tomochika Kurita, Yoshihiko Nishimori, Fumiyuki Toshimitsu, Satoshi Muratsugu, Shoko Kume, and Hiroshi Nishihara*

Department of Chemistry, Graduate School of Science, University of Tokyo, Hongo, Bunkyo-ku, Tokyo 113-0033, Japan

Received December 11, 2009; E-mail: nisihara@chem.s.u-tokyo.ac.jp

One goal of molecular electronics is to control electron conduction in molecular wires and networks by combining appropriate molecular units.[1] A requisite for constructing molecular electronic devices is the connection of molecular wires to the electrode surface. Thus, to evaluate the total performance of the molecular wires as well as the conventional electronic circuit, the electron conduction properties of internal molecular segments as well as the resistivity at the electrode−molecular wire junction must be elucidated.[2] Hence, the surface junction is a fundamentally important issue in the performance of organic thin-film field-effect transistors and light-emitting diode devices.[3]

Stepwise coordination reactions to lengthen molecular wires have recently attracted much attention as a convenient method to connect molecular wires to the surface because these reactions are programmable and connect different units at the desired positions.[4] We previously reported the synthesis of π-conjugated linear and branched M(tpy)$_2$ (M = Fe, Co; tpy = 2,2′:6′,2″-terpyridine) oligomer wires attached to Au using the stepwise coordination method[5] and clarified that the redox conduction of the Fe(tpy)$_2$ oligomer films occurs along the molecular wires,[5c] implying that intrawire electron transfer is much faster than interwire transfer. Additionally, we found that the M(tpy)$_2$ oligomer wires show superior long-range electron-transport abilities.[5e]

In the present study, we used the stepwise coordination method to construct a system to clarify how the electron transport behavior of molecular wires depends on the surface junction at the molecular level by changing only the surface-anchoring molecular unit. Herein we describe the dependence of the electron transfer rate constant, k_{et}, and the electron transport ability of *p*-phenylene-bridged Fe(tpy)$_2$ oligomer wires on three surface-anchoring tpy ligands. Although the three anchoring ligands give the same value of β[d], which indicates the degree of reduction of k_{et} with wire length, the significant difference in the k_{et} values is due to the electronic and steric factors of the surface-anchoring ligands.

As reported previously, $[Fe^{II}(tpy)_2]^{2+}$ oligomer wires with BF_4^- counterions were prepared by a simple bottom-up method using a stepwise complexation reaction (Figure 1A).[5] To construct molecular wires on gold/mica, designated as Au−[**A**^{x}**(FeL)**$_{n-1}$**FeT**] (x = 1, 2, 3), where n is the number of Fe(tpy)$_2$ units, we employed disulfide derivatives of azobenzene-linked tpy (**A**$^1_2$), phenylene-linked tpy (**A**$^2_2$), and a bulky *t*-Bu$_2$Ph-substituted phenylene-linked tpy (**A**$^3_2$) as surface-anchoring ligands, tpy−C$_6$H$_4$−tpy (**L**) as the bridging ligand, and tpy−C≡C−Fc (**T**; Fc = ferrocenyl) as the terminal ligand (Figure 1B). The disulfide derivative **A**$^3_2$ was newly prepared (see the Supporting Information).

Quantitative accumulation of each fragment by stepwise coordination was confirmed by infrared reflection absorption spectroscopy (IRRAS), contact angle measurements, and cyclic voltammetry. Comparison of the IRRAS results for each step in the preparation of Au−[**A**^{3}**(FeL)**$_4$**FeT**] with reference spectra of **A**^{3}, **L**, and **T** revealed that the intensities of the peaks at 1080, 1430, and 1610 cm^{-1} increased with increasing accumulation (Figures S1 and S2 in the Supporting Information); these peaks are attributed to B−F stretching in BF_4^-, C=C stretching in tpy, and C=N stretching in tpy, respectively. The peak at 2200 cm^{-1} in the film spectrum after connection of the terminal ligand **T** is ascribed to the C≡C stretching vibration.

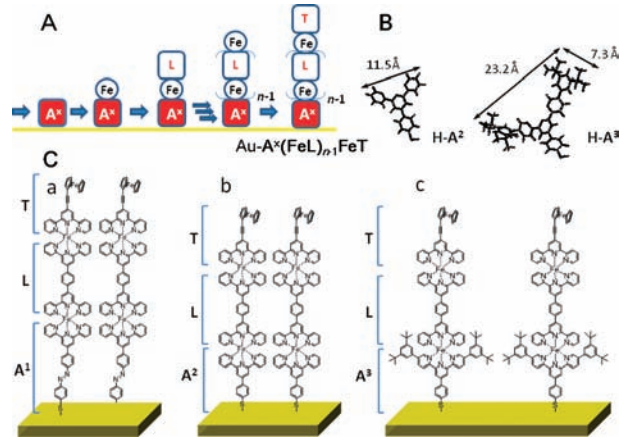

Figure 1. (A) Bottom-up construction of a metal-complex oligomer wire, Au−[**A**^{x}**(FeL)**$_{n-1}$**FeT**]. (B) Molecular sizes of H−**A**^{2} and H−**A**^{3} estimated from DFT calculations. (C) Chemical structures of Au−[**A**^{x}**FeLFeT**] molecular wires with (a) x = 1, (b) x = 2, and (c) x = 3.

The contact angles of water droplets on the films were measured at each step of the coordination reactions. The films with **A**^{1} and **A**^{2} showed similar variations in the contact angle as the structure was formed, whereas the film with **A**^{3} exhibited a different behavior (Figure S3). The contact angle immediately after attachment of a surface ligand was larger for **A**^{3} than for **A**^{1} or **A**^{2}, probably because of the effect of the hydrophobic *t*-Bu$_2$Ph moieties in **A**^{3}. The contact angle decreased when a ferrous ion was attached and increased upon attachment of an **L** ligand, as expected from the hydrophilicity of the ferrous ion and the hydrophobicity of **L**. The overall change in the contact angle was greater for **A**^{3} than for **A**^{1} or **A**^{2}, and the contact angles of all three films approached a similar value at the end of the reactions. This finding is reasonable because all three cases are expected to produce similar surface structures.

In the cyclic voltammograms (CVs) of Au−[**A**^{x}**(FeL)**$_{n-1}$**FeT**], the ferrocenium/ferrocene (Fc^+/Fc) redox couple in **T** was observed at $E^{0'}$ = 0.08−0.11 V versus Fc^+/Fc, and the $Fe^{III}(tpy)_2/Fe^{II}(tpy)_2$ couple was observed at $E^{0'}$ = 0.64−0.65 V versus Fc^+/Fc. These values depended slightly on both x and n because of the electron-donating and -withdrawing effects of the substituents on the Fe(tpy)$_2$ moiety (Figures S4−S7). The amounts of terminal ferrocene units in the molecular wire films, Γ, were evaluated from the CVs to be 1.7×10^{-10}, 1.4×10^{-10}, and 6.0×10^{-11} mol cm^{-2} for the films with x = 1, 2, and 3, respectively. The smaller Γ value for the **A**^{3} film is reasonable because the **A**^{3} is larger than **A**^{1} and **A**^{2} as a result of the existence of the two *t*-Bu$_2$Ph moieties on the tpy unit.

10.1021/ja910462x

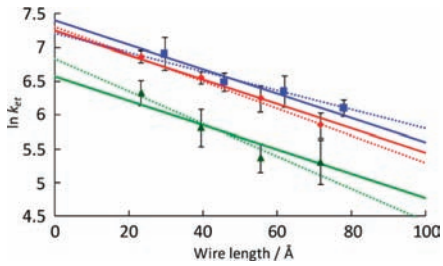

Figure 2. Plots of ln(k_{et}) vs d for **[A^x(FeL)$_{n-1}$FeT]** (blue, $x = 1$; green, $x = 2$; red, $x = 3$). Dashed lines were obtained by least-squares fitting for each x and solid lines by fitting for all x assuming the same slope.

The areas occupied by single Au−[**A^2(FeL)FeT**] and Au−[**A^3(FeL)FeT**] wires were evaluated by density functional theory (DFT) calculations to be 100 and 250 Å^2, respectively; these correspond to densities of 1.7×10^{-10} mol cm^{-2} and 6.8×10^{-11} mol cm^{-2}, suggesting that the molecular wires are relatively densely packed on the surface. The number of Fe(tpy)$_2$ units in the film increased linearly with the number of coordination cycles, as reported previously,[5] indicating quantitative accumulation of the molecular units.

Rate constants for electron transfer between the electrode and the terminal ferrocene moiety of the molecular wires, k_{et}, were measured for Au−[**A^x(FeL)$_{n-1}$FeT**] ($x = 1, 2, 3$; $n = 1, 2, 3, 4$) by potential-step chronoamperometry for reduction of the terminal ferrocenium moiety at −0.13 V versus Fc$^+$/Fc. Each chronoamperogram showed an exponential decay of current (i) as a function of time (t), and k_{et} was obtained from the slope of the plot of ln(i) versus t. From the relationship of k_{et} to the length of the molecular wire between the electrode surface and the Fe center in the terminal ferrocenium moiety, d, we estimated β^d and k_{et}^0 using eq 1:

$$k_{et} = k_{et}^0 \exp[-\beta^d(d - d^0)] \quad (1)$$

where d^0 is the shortest molecular length (when $n = 1$) and k_{et}^0 is the k_{et} value at d^0. Least-squares fits of the plots gave $\beta^d = 0.014 \pm 0.004$, 0.024 ± 0.007, and 0.020 ± 0.004 for the wires with **A^1**, **A^2**, and **A^3**, respectively (see Figure 2). We also fitted straight lines with the same slope to the plots (see Figure 2) in order to analyze the results using the same values of β^d for all three types of molecular wires. This analysis is reasonable because the metal complex wire and the terminal redox-active moiety were kept constant and only the surface-attaching ligand was changed. The value of β^d thus evaluated was 0.018, which is consistent with a previous result.[5e]

The three lines in Figure 2 are parallel but shifted vertically depending on the surface-anchoring ligand. For a given x, the wires with **A^2** have a much lower value of k_{et} than do wires with **A^1**, despite the shorter surface-anchoring ligand; the value with **A^2** is also smaller than that for wires with **A^3**, despite a similar p-phenylene-bridged structure and thus similar d^0.

Molecular orbital (MO) calculations for H−**A^{x}Fe(tpy)** ($x = 1$, 2, 3) were performed using DFT to elucidate the electronic effects on k_{et} (Figures S8−S12). The electronic structure of azobenzene-bridged **A^1** differs from that of p-phenylene-bridged **A^2** in the following two ways: (1) one MO (orbital 179) extends over the terminal SH moiety, the azobenzene bridge, and the Fe center; (2) there are MOs attributed to the azobenzene moiety around the HOMO (orbitals 180−184). These results indicate that the azobenzene moiety can promote stronger electron coupling between the surface Au−S and the nearest Fe(tpy)$_2$ unit and thus increase the electron conduction rate in the molecular wire. In contrast, H−**A^{2}Fe(tpy)** and H−**A^{3}Fe(tpy)** have similar electronic structures, and in both, the HOMO is localized at the phenylene moiety (orbitals 157 and 261, respectively) and MOs near the Fe center are below the HOMO (orbitals 153−156 and 253−256, respectively). The energies of these orbitals are slightly higher for H−**A^{3}Fe(tpy)** because of the electron-donating effect of the t-Bu$_2$Ph groups. Although the electronic effect may contribute to some extent to the significant difference in the k_{et}^0 values, the steric effect of the t-Bu$_2$Ph groups is likely to have more influence on this difference. As noted above, the molecular wires in the film containing **A^3** have a lower value of Γ than do the molecular wires in the film containing **A^2**, indicating that electrolyte ions can come closer to the electrode surface in the film containing **A^3** than in the film with **A^2**. In fact, the electron transfer rate constant for the $[Fe(tpy)_2]^{3+}/[Fe(tpy)_2]^{2+}$ couple was higher for Au−[**A^{3}FeL**] (330 s^{-1}) than for Au−[**A^{2}FeL**] (56 s^{-1}) (Figures S13 and S14).

In conclusion, the surface-anchoring molecular unit does not affect the dependence of the electron transport properties of the molecular wire on the wire length, but it alters the absolute rate constant. This finding indicates that the electron conduction kinetics of molecular wires on the surface can be tuned by varying the combination of the surface-anchoring and internal units of the molecular wire. The confirmation of this fundamental issue of molecular-wire electron conduction will contribute significantly to developing the field of molecular electronics.

Acknowledgment. This work was supported by Grants-in-Aid from MEXT of Japan (20245013 and 21108002, Area 2107) and the Global COE Program for Chemistry Innovation.

Supporting Information Available: Materials and methods, electrochemical and spectral data, and results of molecular orbital calculations. This material is available free of charge via the Internet at http://pubs.acs.org.

References

(1) (a) Joachim, C.; Gimzewski, J. K.; Aviram, A. *Nature* **2000**, *408*, 541. (b) Park, J.; Pasupathy, A. N.; Goldsmith, J. I.; Chang, C.; Yaish, Y.; Petta, J. R.; Rinkoski, M.; Sethna, J. P.; Abruña, H. D.; McEuen, P. L.; Ralph, D. C. *Nature* **2002**, *417*, 722. (c) Welter, S.; Brunner, K.; Hofstraat, J. W.; Cola, L. D. *Nature* **2003**, *421*, 54. (d) Chidsey, E. D.; Murray, R. W. *Science* **1986**, *231*, 25. (e) Wrighton, M. S. *Science* **1986**, *231*, 32. (f) Wenger, O. S.; Leigh, B. S.; Villahermosa, R. M.; Gray, H. B.; Winkler, J. R. *Science* **2005**, *307*, 99. (g) Xu, B.; Tao, N. J. *Science* **2003**, *301*, 1221. (h) Nitzan, A.; Ratner, M. A. *Science* **2003**, *300*, 1384. (i) Choi, S. H.; Kim, B.-S.; Frisbie, C. D. *Science* **2008**, *320*, 1482.

(2) (a) Park, Y. S.; Whalley, A. C.; Kamenetska, M.; Steigerwald, M. L.; Hybertsen, M. S.; Nuckolls, C.; Venkataraman, L. *J. Am. Chem. Soc.* **2007**, *129*, 15768. (b) Tsutsui, M.; Taniguchi, M.; Kawai, T. *J. Am. Chem. Soc.* **2009**, *131*, 10552.

(3) (a) Terada, K.; Kobayashi, K.; Hikita, J.; Haga, M. *Chem. Lett.* **2009**, *38*, 416. (b) Chan, I.-M.; Hong, F. C. *Thin Solid Films* **2004**, *450*, 304.

(4) (a) Abe, M.; Michi, T.; Sato, A.; Kondo, T.; Zhou, W.; Ye, S.; Uosaki, K.; Sasaki, Y. *Angew. Chem., Int. Ed.* **2003**, *42*, 2912. (b) Wanunu, M.; Vaskevich, A.; Cohen, S. R.; Cohen, H.; Arad-Yellin, R.; Shanzer, A.; Rubinstein, I. *J. Am. Chem. Soc.* **2005**, *127*, 17877. (c) Jiao, J.; Anariba, F.; Tiznado, H.; Schmidt, I.; Lindsey, J. S.; Zaera, F.; Bocian, D. F. *J. Am. Chem. Soc.* **2006**, *128*, 6965. (d) Such, G. K.; Quinn, J. F.; Quinn, A.; Tjipto, E.; Caruso, F. *J. Am. Chem. Soc.* **2006**, *128*, 9318. (e) Altman, M.; Shukla, A. D.; Zubkov, T.; Evmenenko, G.; Dutta, P.; van der Boom, M. E. *J. Am. Chem. Soc.* **2006**, *128*, 7374. (f) Wanunu, M.; Vaskevich, A.; Shanzer, A.; Rubinstein, I. *J. Am. Chem. Soc.* **2006**, *128*, 8341. (g) Kanaizuka, K.; Haruki, R.; Sakata, O.; Yoshimoto, M.; Akita, Y.; Kitagawa, H. *J. Am. Chem. Soc.* **2008**, *130*, 15778. (h) Kosbar, L.; Srinivasan, C.; Afzali, A.; Graham, T.; Copel, M.; Krusin-Elbaum, L. *Langmuir* **2006**, *22*, 7631.

(5) (a) Kanaizuka, K.; Murata, M.; Nishimori, Y.; Mori, I.; Nishio, K.; Masuda, H.; Nishihara, H. *Chem. Lett.* **2005**, *34*, 534. (b) Ohba, Y.; Kanaizuka, K.; Murata, M.; Nishihara, H. *Macromol. Symp.* **2006**, *235*, 31. (c) Nishimori, Y.; Kanaizuka, K.; Murata, M.; Nishihara, H. *Chem.—Asian J.* **2007**, *2*, 367. (d) Utsuno, M.; Toshimitsu, F.; Kume, S.; Nishihara, H. *Macromol. Symp.* **2008**, *270*, 153. (e) Nishimori, Y.; Kanaizuka, K.; Kurita, T.; Nagatsu, T.; Segawa, Y.; Toshimitsu, F.; Muratsugu, S.; Utsuno, M.; Kume, S.; Murata, M.; Nishihara, H. *Chem.—Asian J.* **2009**, *4*, 1361.

JA910462X